CHAPTER V

RESULTS AND DISCUSSION

5.1 Characterization of Catalyst

Crystal structures of prepared catalysts were analysed by XRD technique. The XRD patterns are report in section 5.1.1, Surface areas are reported in section 5.1.2. Scanning electron microscope photos are exhibited in section 5.1.3.

5.1.1 X-Ray Diffraction Patterns

1. H-ZSM-5
2. H-Fe-Silicate
3. H-Zn-Silicate
4. Fe/H-ZSM-5 (5 wt % Fe)
5. Zn/H-ZSM-5 (5 wt % Zn)
6. H-Fe.Al-silicate
7. H-Zn.Al-silicate

The X-ray diffraction patterns for the catalysts prepared and H-ZSM-5 of patent literature are shown in Figure 5.1. The patterns of catalysts, prepared in this laboratory by rapid crystallization method, were the same as that of H-ZSM-5. This indicates that all the prepared catalysts have the same pentasil pore-opening structure as H-ZSM-5. Consequently, both the metals incorporated and the metals ion-exchanged do not change the structure of H-ZSM-5 catalyst.

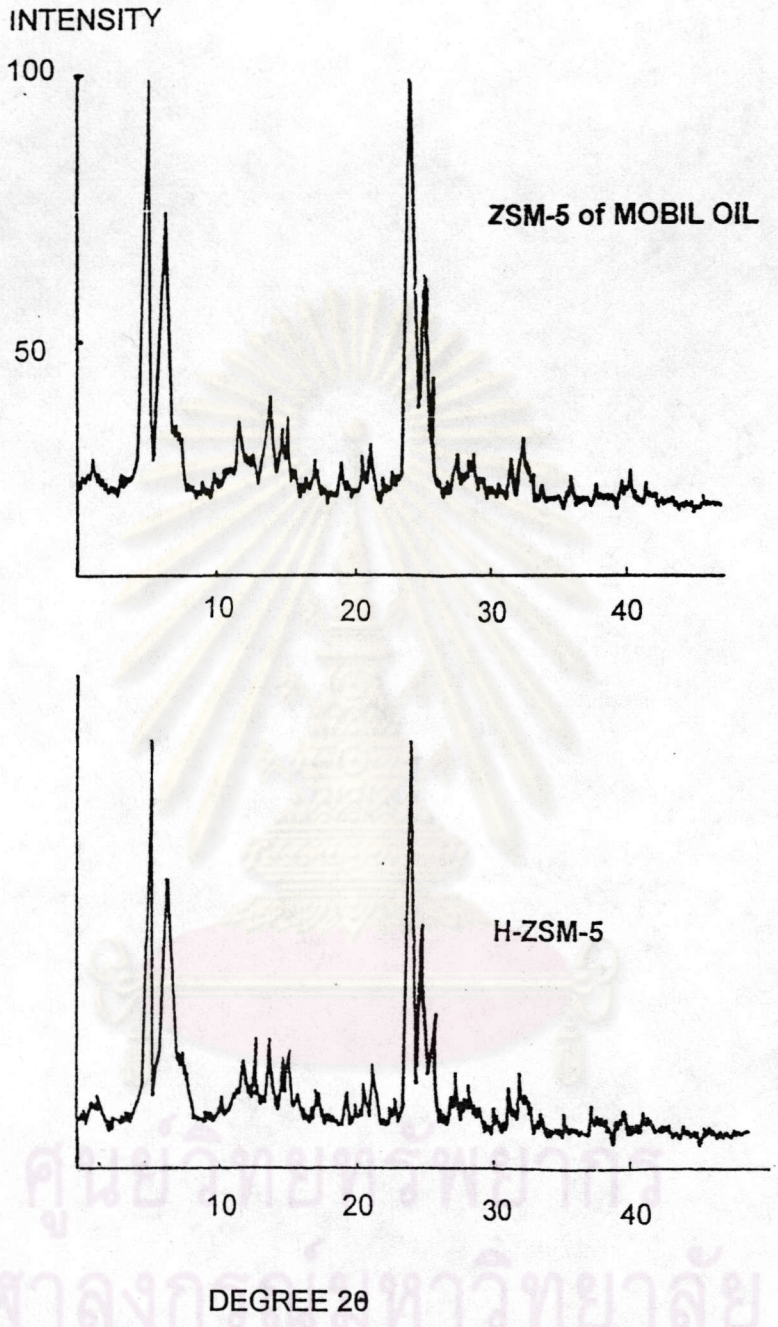

Figure 5.1 X-ray diffraction patterns of the catalysts.

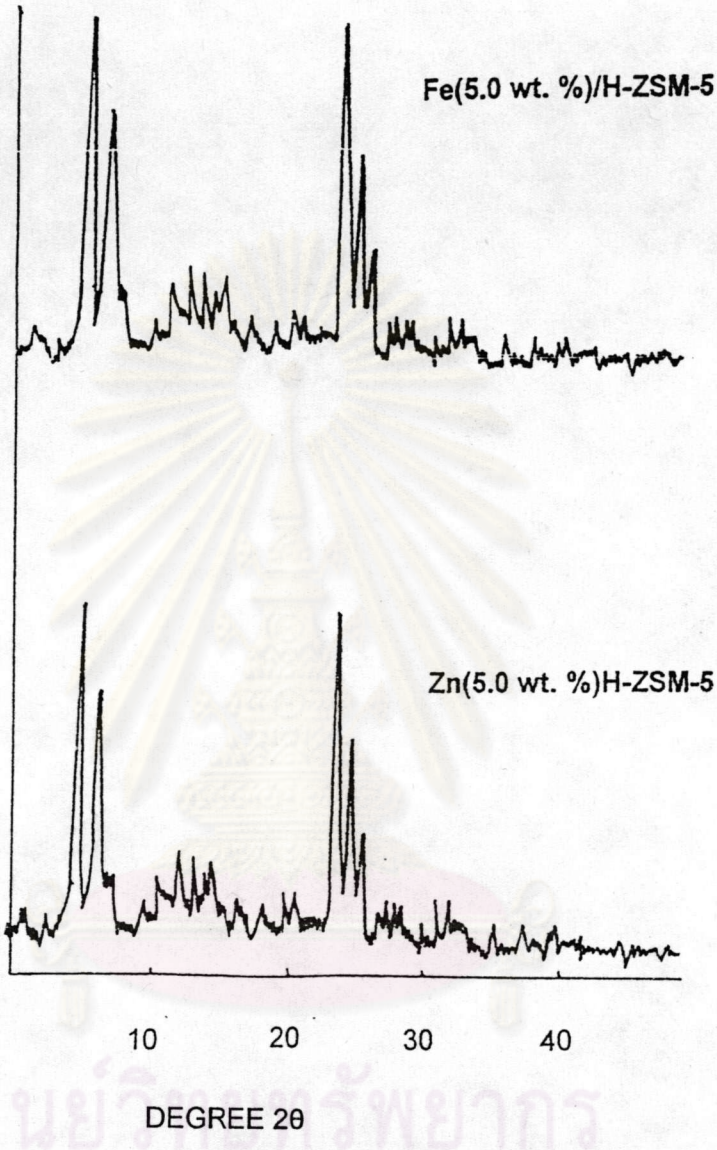

Figure 5.1 X-ray diffraction patterns of the catalysts (continued).

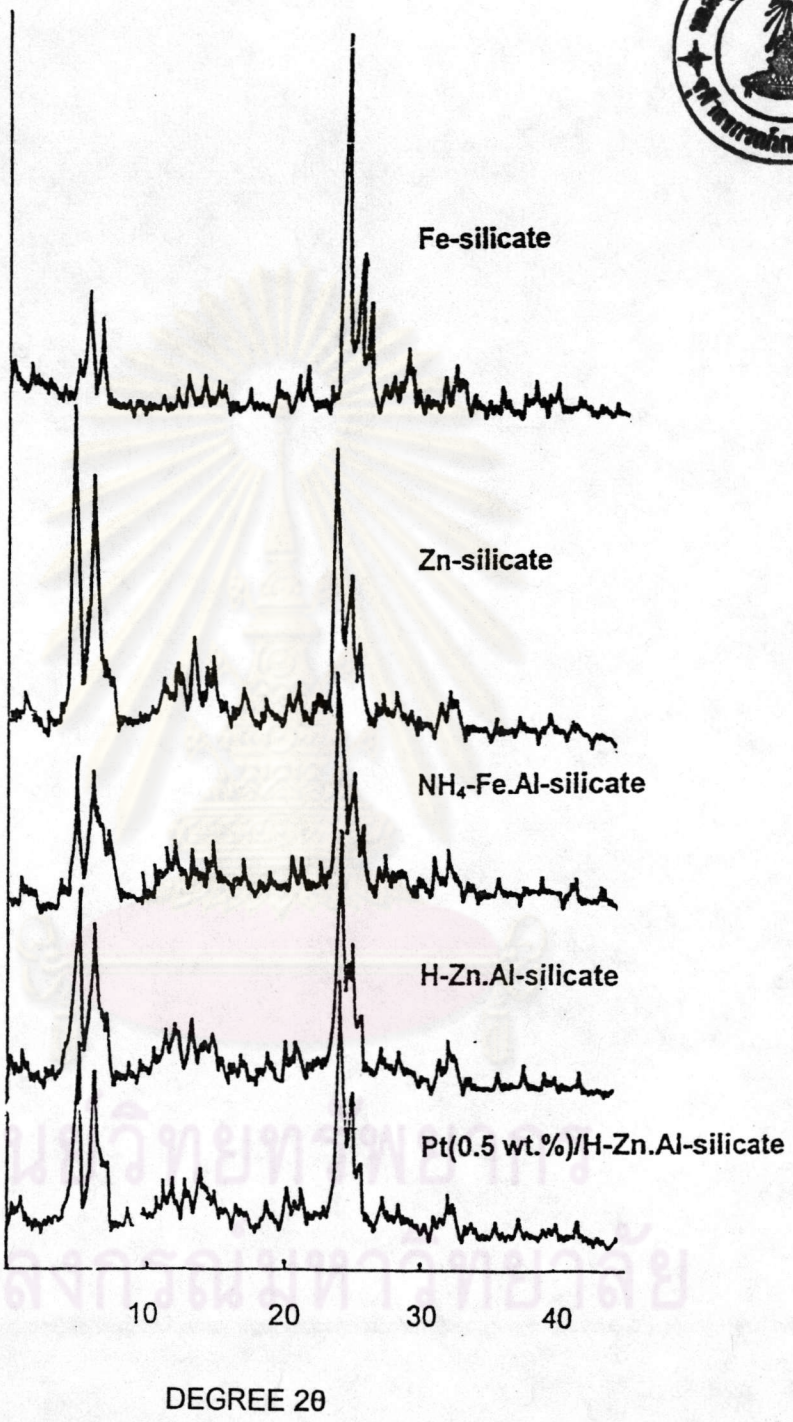

Figure 5.1 X-ray diffraction patterns of the catalysts (continued).

5.1.2 Specific Surface Area

BET surface areas of the catalysts are show in Table 5.1. The surface areas of all metal ion-exchanged ZSM-5, iron incorporated and zinc incorporated catalysts were in the same range as that of H-ZSM-5. This is consistent with the above-mentioned result that the XRD patterns of all the prepared catalysts are almost the same as that of H-ZSM-5. The only exceptions is H-Fe-Silicate and H-Zn-Silicate which have lower surface area.

Table 5.1 BET surface areas of the catalysts.

Catalysts	BET surface areas (m^2/g of catalyst)
H-ZSM-5	382.1762
H-Fe-Silicate	267.1759
H-Zn-Silicate	274.4740
(5 wt %) Fe/H-ZSM-5	338.3268
(5 wt %) Zn/H-ZSM-5	356.4531
NH_4-Fe/Al-Silicate	365.2463
H-Zn/Al-Silicate	400.4378
Pt/H-Zn.Al-silicate (0.5 wt % pt)	341.0235

5.1.3 Morphology

Scanning electron microscope photographs of the catalysts are shown in Figure 5.2. As shown, the crystal shape and size of metal loaded catalysts (Fe, Zn)

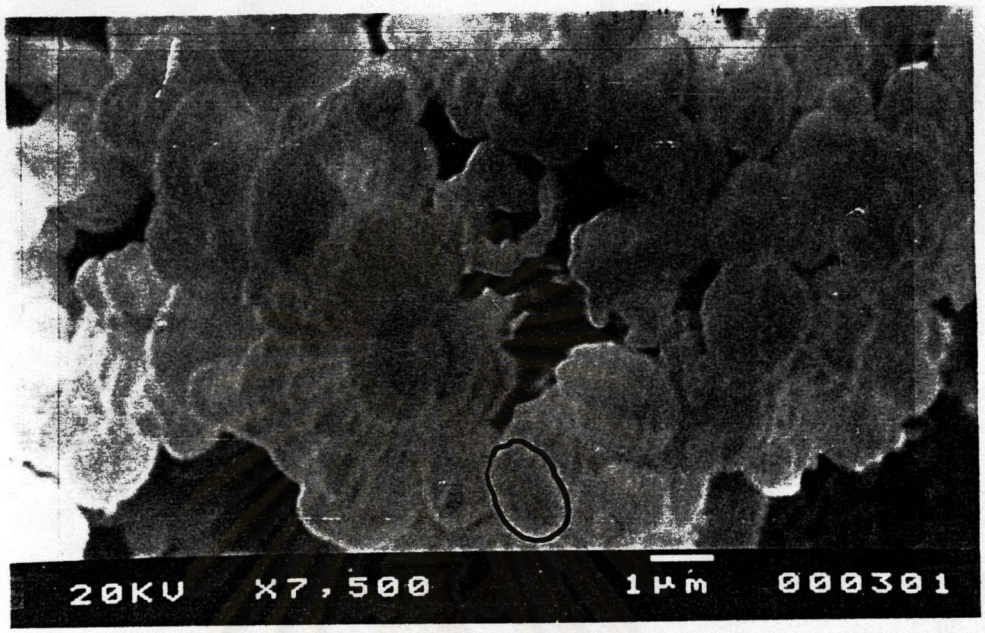

a) H-ZSM-5

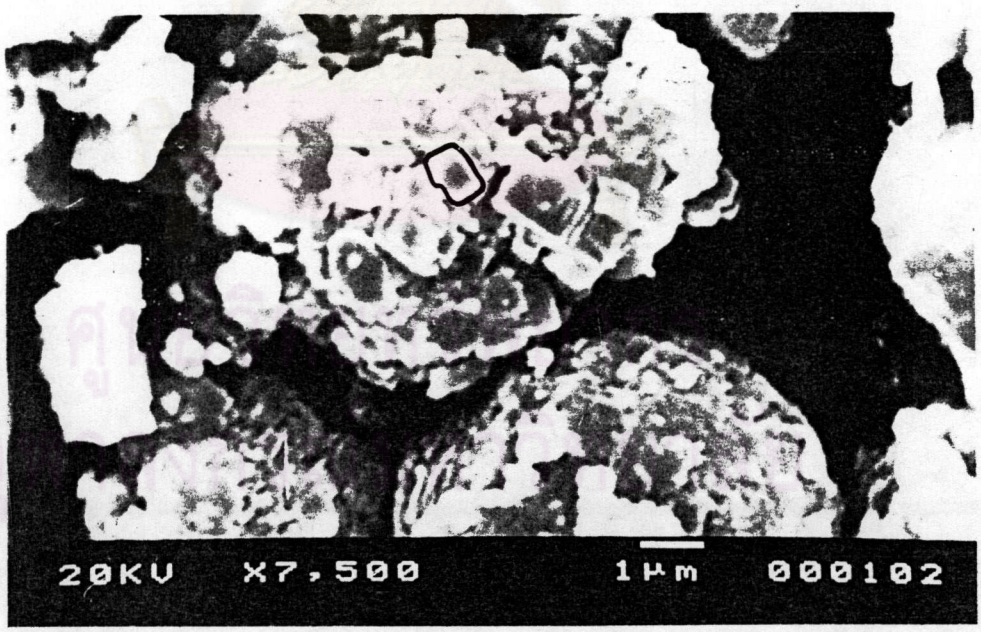

b) H-Fe-Silicate

Figure 5.2 SEM Photographs of the catalysts.

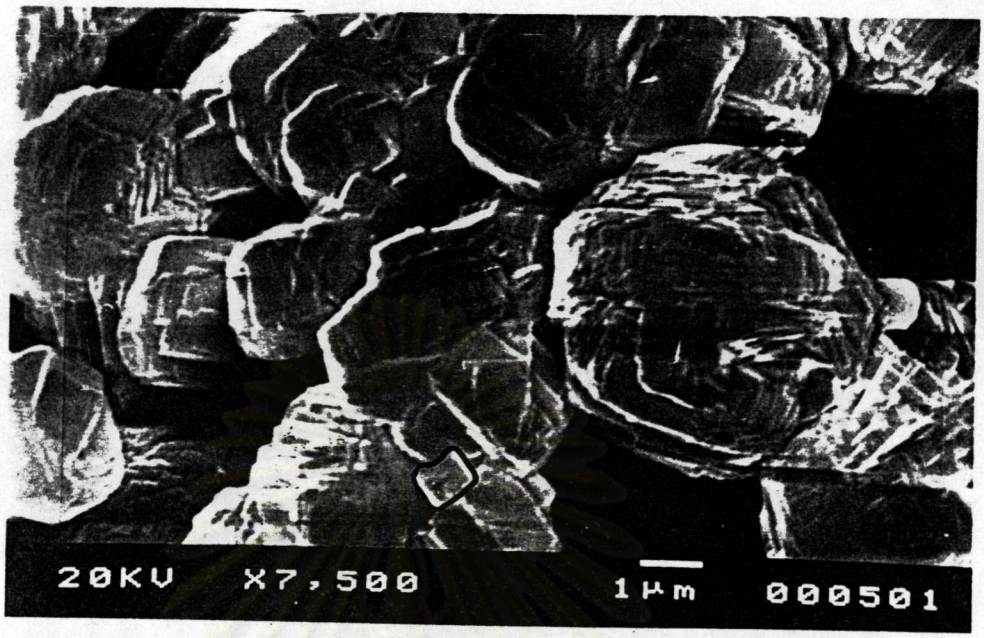

c) H-Zn-Silicate

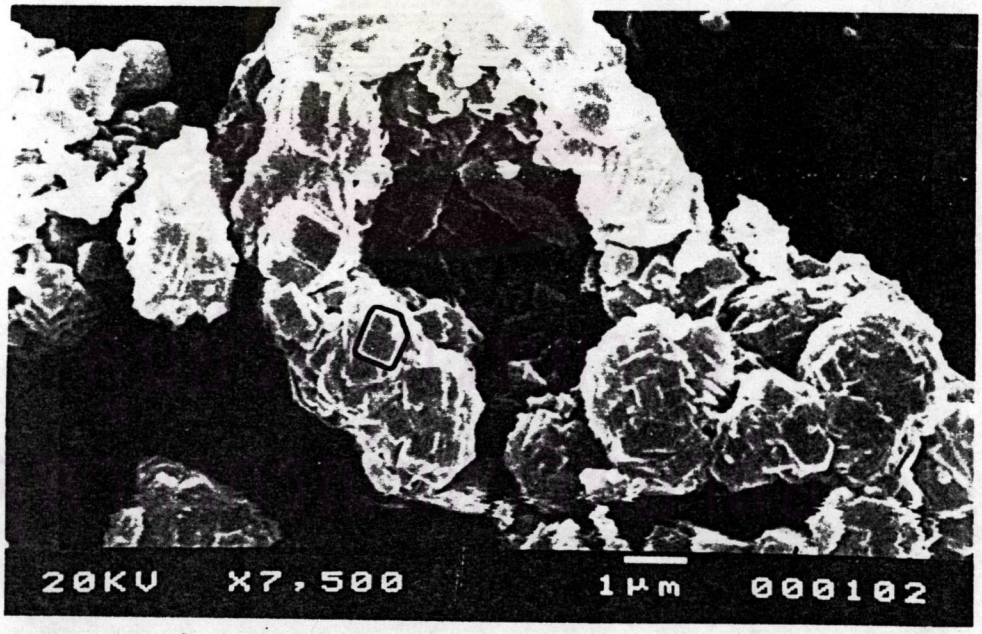

d) Fe/H-ZSM-5 (5 wt% Fe)

Figure 5.2 SEM Photographs of the catalysts. (continued)

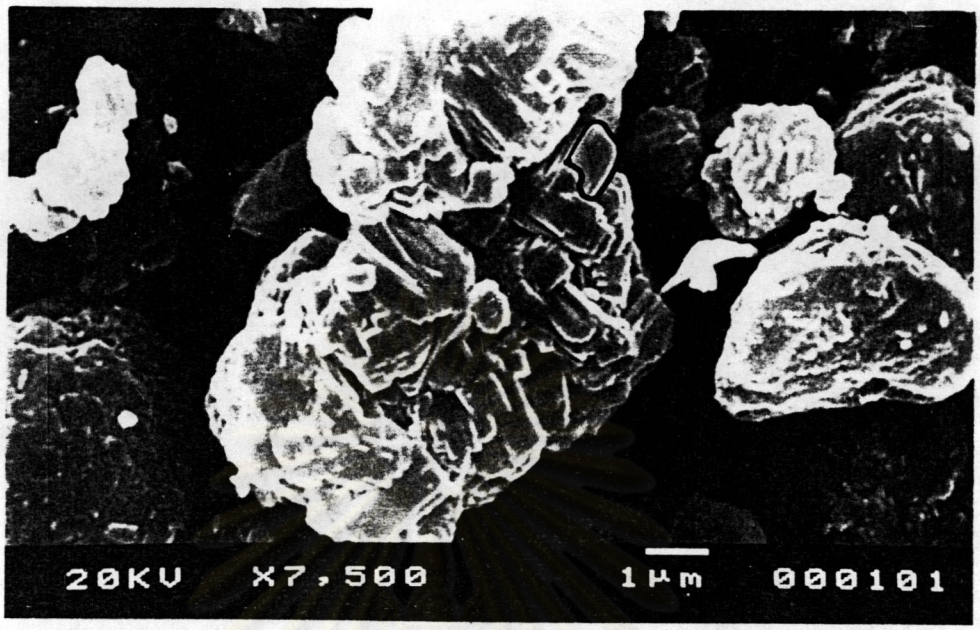

e) Zn/H-ZSM-5 (5 wt% Zn)

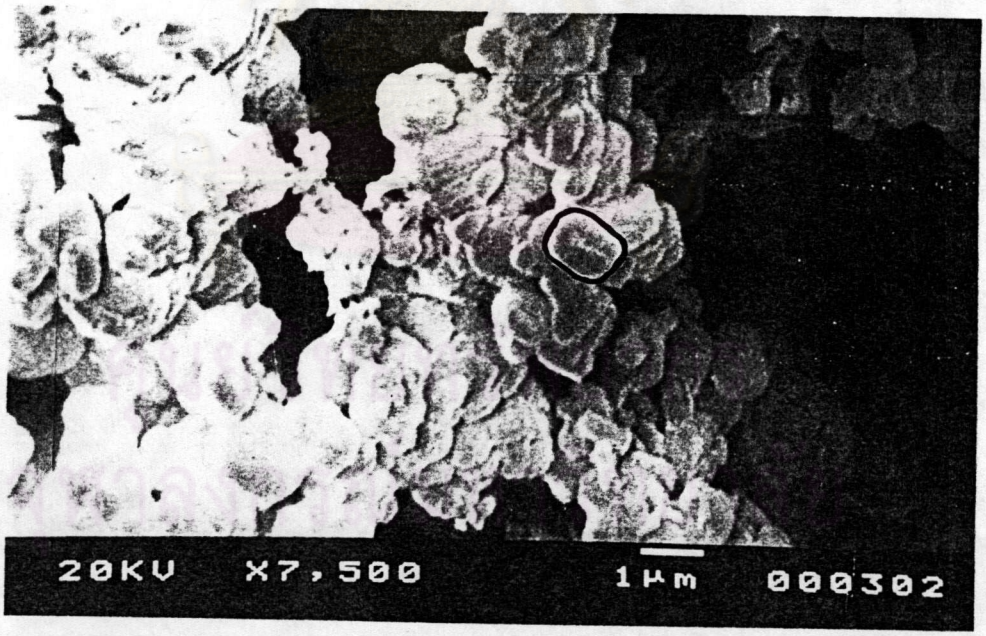

f) NH_4-Fe-Al-Silicate

Figure 5.2 SEM Photographs of the catalysts. (continued)

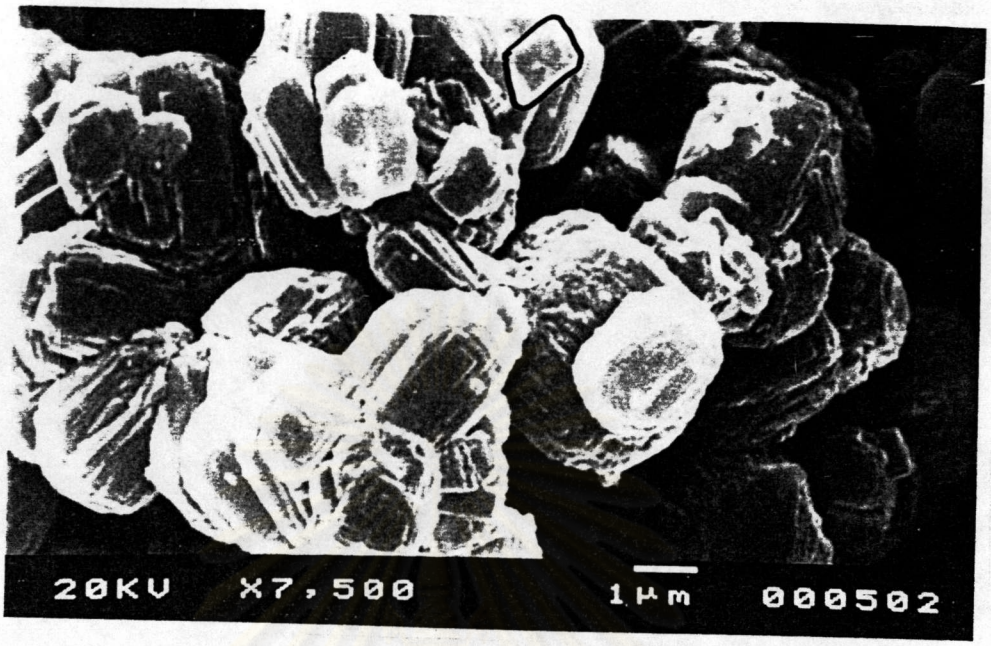

g) H-Zn-Al-Silicate

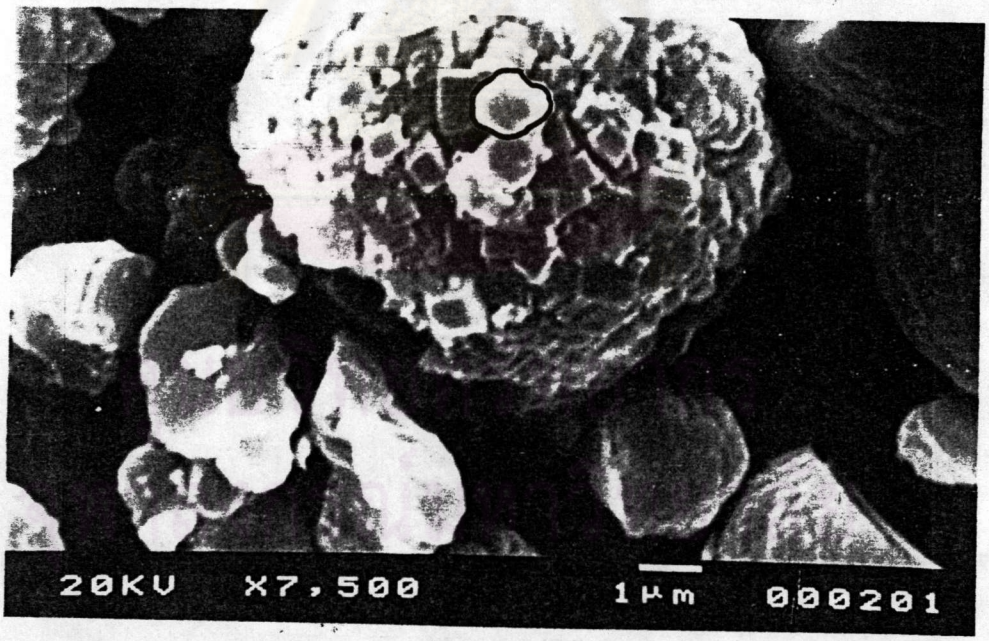

h) Pt/H-Zn-Al-Silicate

Figure 5.2 SEM Photographs of the catalysts. (continued)

were identical with the parent H-ZSM-5 and conformed to their characteristics of catalysts on figure 5.2

Methanol conversion to aromatics reaction

5.1.4 Effect of NH_4^+ Form and H-Form ZSM-5

The methanol conversion to hydrocarbons was carried out at GHSV 2000 h^{-1}, temperature 350° C, feed gas mixture of 20% MeOH balanced with 80% N_2 and 1 hr. on stream. Compared between NH_4^+ form and H form of ZSM-5, light olefins and aromatics selectivity were not so different which are shown in Figure 5.3. These results were used as the reference for the modification of various metal into framework of ZSM-5.

5.1.5 Methanol conversion on Fe-silicate catalysts

Effect of Fe amounts in Fe-silicate catalyst on hydrocarbon distribution (Si/Fe=25, Si/Fe=40 and Si/Fe=400) are shown in Figure 5.4. All the catalysts exhibited high selectivity to light olefins, which is slightly decreased with increasing Si/Fe ratio in the catalyst and the selectivity for aromatics was considerably low. As for the catalyst of Si/Fe=25, the methanol conversion was 43.20 % with the light olefins selectivity of 43.68 %. The methanol was completely converted to hydrocarbon on the catalyst of Si/Fe=40 and the methanol conversion slightly reduced to about 80 % on Si/Fe=400. The considerably low selectivity for aromatics should be attributed to the weaker acidity of Fe-silicate catalyst than H-ZSM-5.

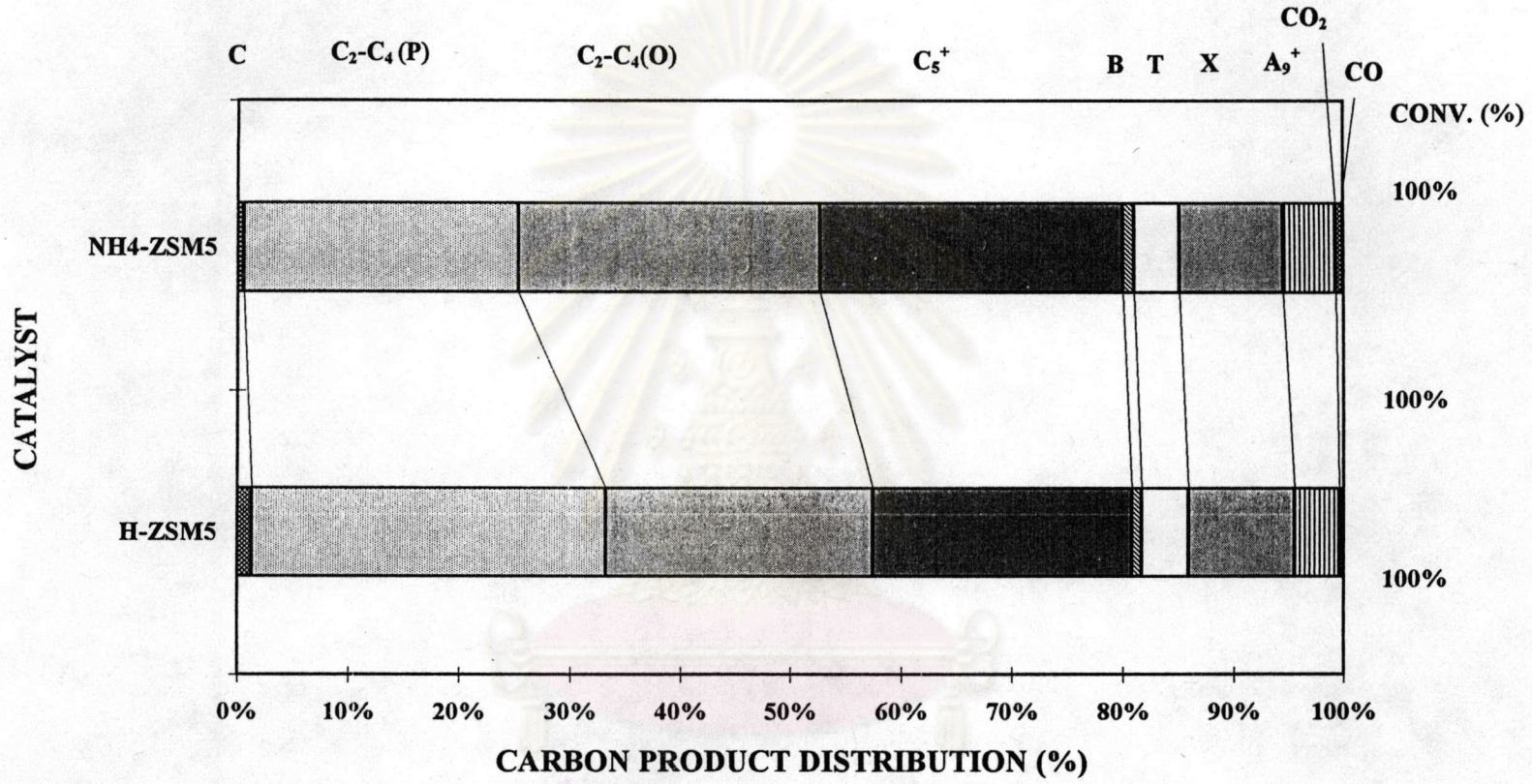

Figure 5.3 Methanol conversion on H-and NH_4-ZSM-5 catalysts.

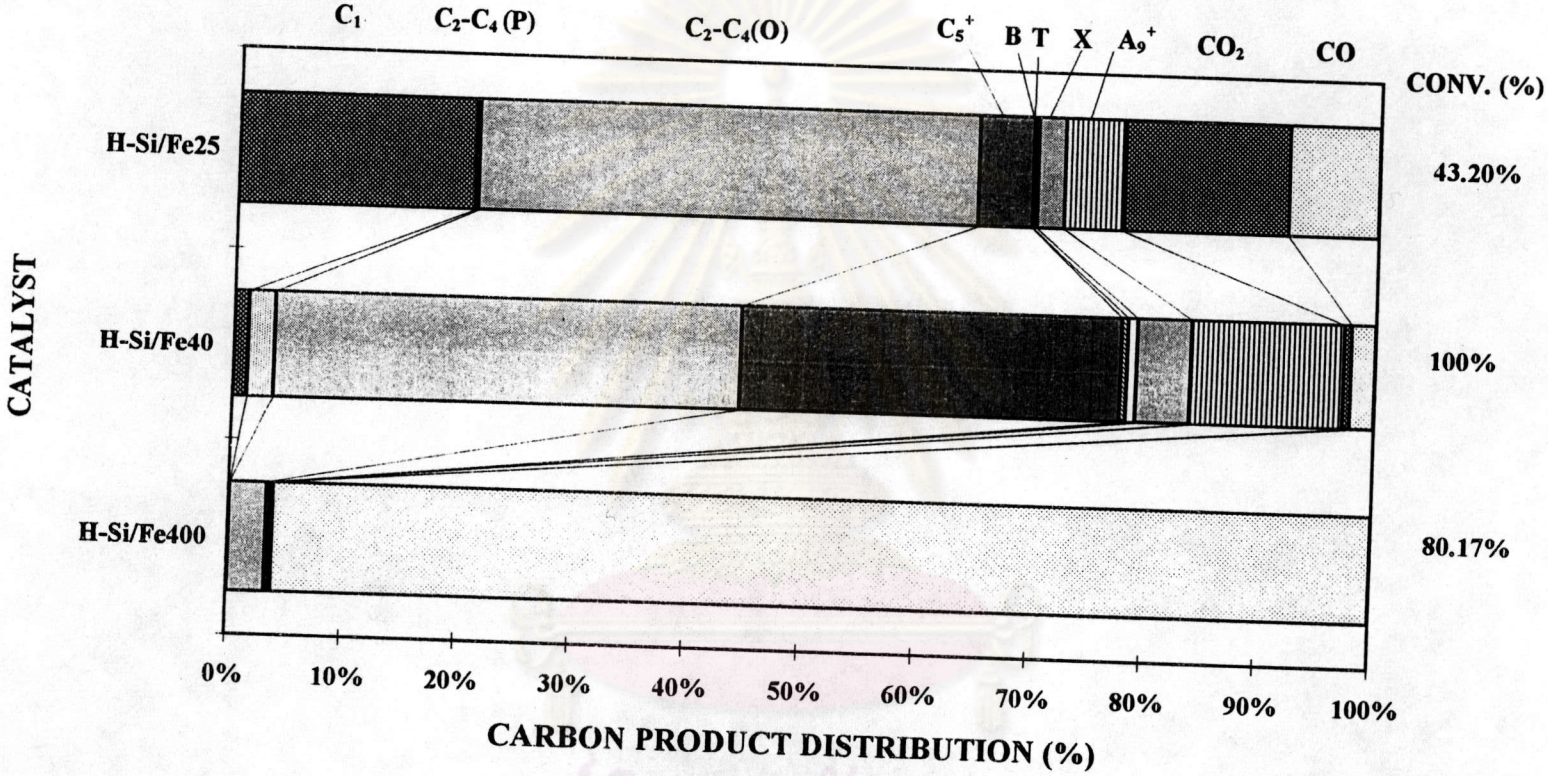

Figure 5.4 Methanol conversion on H-Fe-silicate catalysts with various Fe loading content.

5.1.6 Methanol conversion on Fe ion-exchanged H-ZSM-5

Hydrocarbon distribution of methanol conversion, with the same condition as mentioned above, on Fe ion-exchanged H-ZSM-5 catalyst with various amounts of Fe, 3, 5 and 10 wt %, is shown in Figure 5.5. The methanol conversion was 100 % for all percentage of Fe loading. Fe ion-exchanged H-ZSM-5 with 5 wt % Fe loading exhibited the highest amount of light olefins and aromatics compared with 3 and 10 wt % Fe loading. It should be noted that Fe ion-exchanged H-ZSM-5 exhibited much higher aromatics than Fe-silicate. The strong acidity derived from the presence of Al in Fe ion-exchanged H-ZSM-5 should be responsible for the higher aromatics selectivity than that of Fe-silicate.

5.1.7 Methanol conversion on H-Fe.Al-silicate

The product distribution of methanol conversion on H-Fe.Al-silicate with S:/A ratio of 40 and Si/Fe ratios of 25, 40, and 400 is shown in Figure 5.6. All the catalysts yielded small amount of BTX and mainly light olefins were produced. However, among the catalyst tested, H-Fe.Al-silicate with Si/Al and Si/Fe ratios of 40 gave the highest amount of BTX.

5.1.8 Methanol conversion on NH_4-Fe.Al-silicate

The product distribution of methanol conversion on NH_4-Fe.Al-silicate with Si/Al ratio of 40 and Si/Fe ratios of 25, 40, and 400 is shown in Figure 5.7. Surprisingly enough, NH_4-Fe.Al-silicate exhibited higher BTX amount than that of the corresponding H-form. The catalyst with Si/Fe and Si/Al ratios of 40 gave

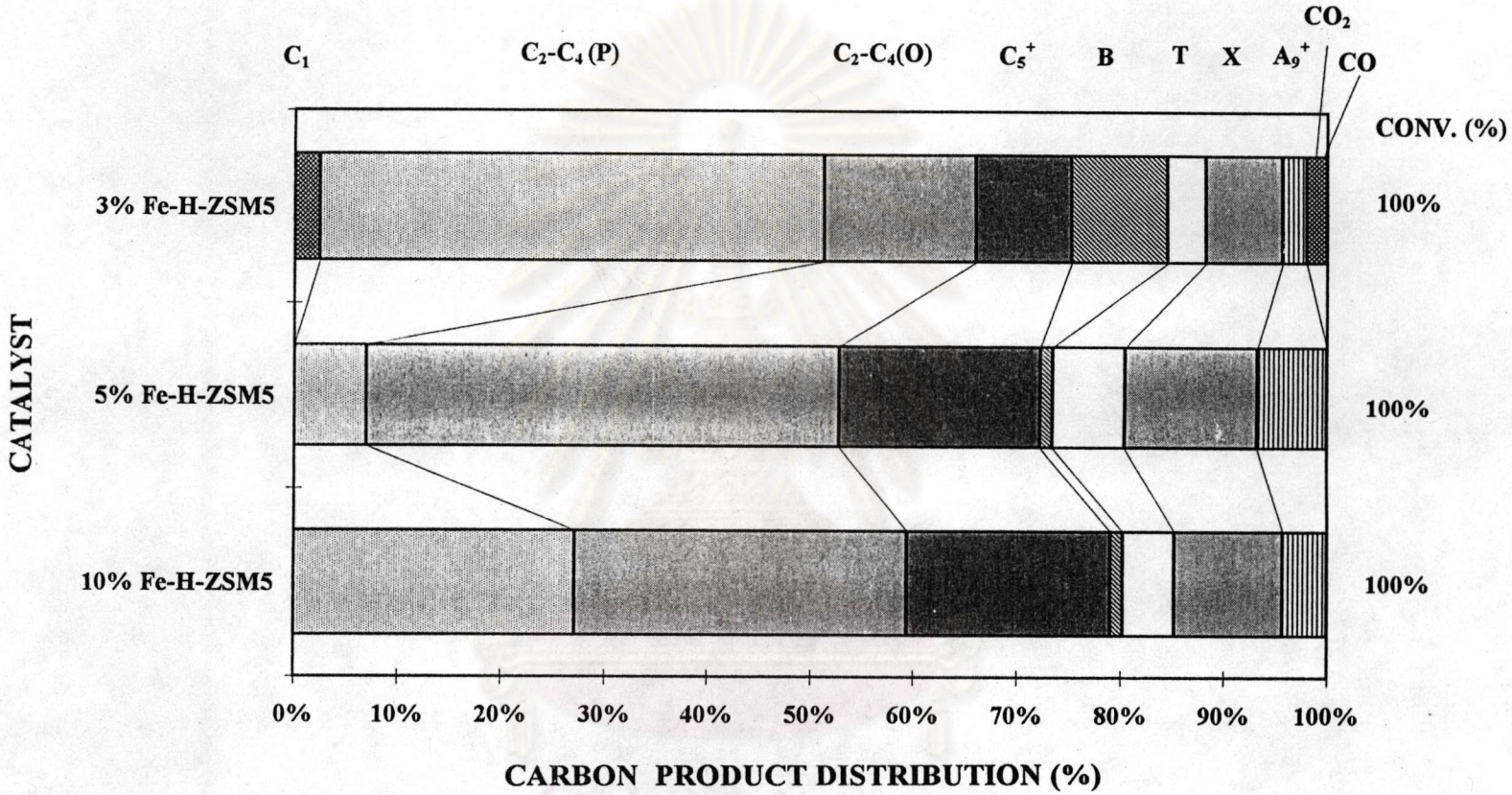

Figure 5.5 Methanol conversion on Fe/H-ZSM-5 catalyst with various Fe loading content.

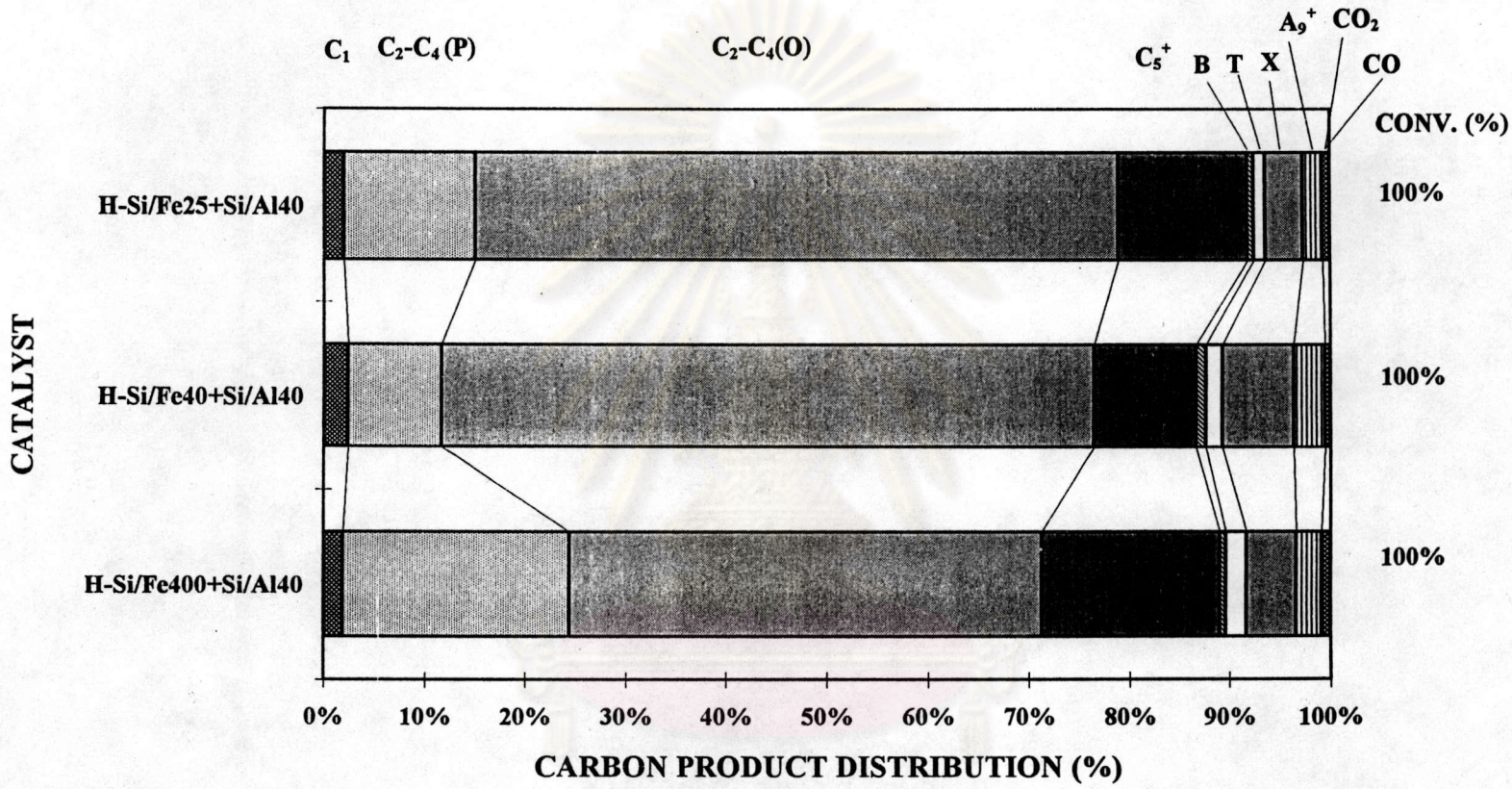

Figure 5.6 Methanol conversion on H-Fe.Al-silicate catalysts with fix Al and various Fe loading content.

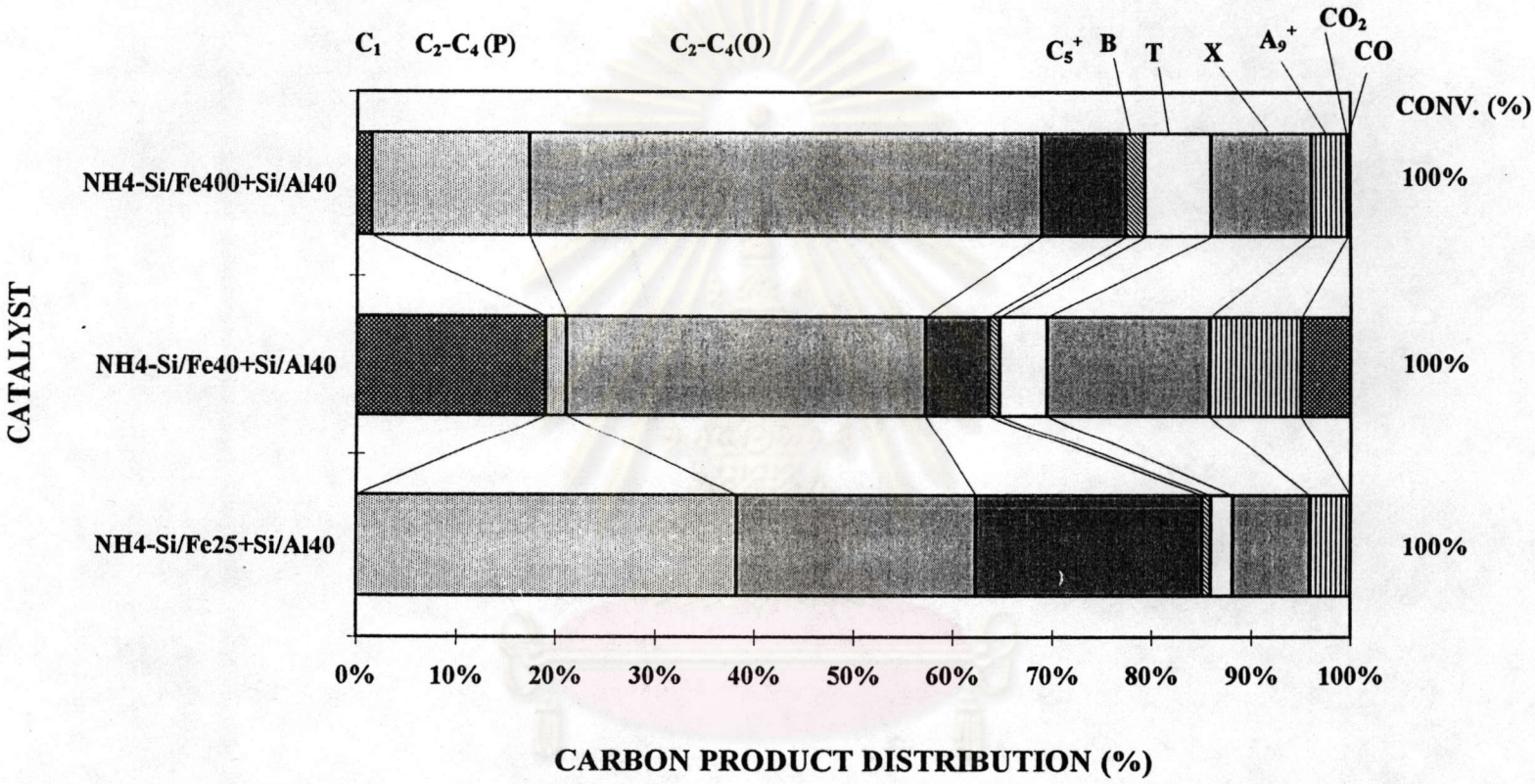

Figure 5.7 Methanol conversion on NH_4-Fe.Al-silicate catalyst with fix Al and various Fe loading content.

approximately 22 % BTX selectivity. It is noteworthy that the cation form does affect the aromatic selectivity though the detailed reason needs further study. The effect of all amount in NH_4-Fe.Al-silicate was also observed and the result is shown in Figure 5.8. Among the catalysts with Si/Al ratios of 25, 40, and 400 at Si/Fe ratio of 40, it has been found that NH_4-Fe.Al-silicate with Si/Al and Si/Fe ratios of 40 was the optimum one for aromatic selectivity.

5.1.9 Methanol conversion on Zn-silicate

The product distribution of methanol conversion on Zn-silicate with Si/Zn ratios of 40 and 400 is shown in Figure 5.9. The catalysts did not give the significant amount of BTX and CO/CO_2 were achieved as the main products. Thus Zn-silicate was not the good catalyst for the aromatization of methanol.

5.1.10 Methanol conversion on Zn ion-exchanged H-ZSM-5

As shown in Figure 5.10, the activity and armatic selectivity were greatly enhanced on Zn ion-exchanged H-ZSM-5. The selectivity for BTX higher than 32 % was achieved during the range of Zn loading from 3 % to 10 %. Zn ion-exchanged H-ZSM-5 with 5 % Zn by weight represents the optimum one.

5.1.11 Methanol conversion on H-Zn.Al-silicate

The product distribution of methanol conversion on H-Zn.Al-silicate is shown in Figure 5.11. First, the Si/Al ratio was fixed at 40 and Si/Zn ratios were varied at 25, 40, and 400. It has been found that H-Zn.Al-silicate with Si/Zn 40 exerted the highest selectivity for BTX of approximately 30 %. Then Si/Zn ratio was thus fixed at 40 and Si/Al ratios were varied at 25, 40, and 400. As shown in figure 5.13, H-Zn.Al-

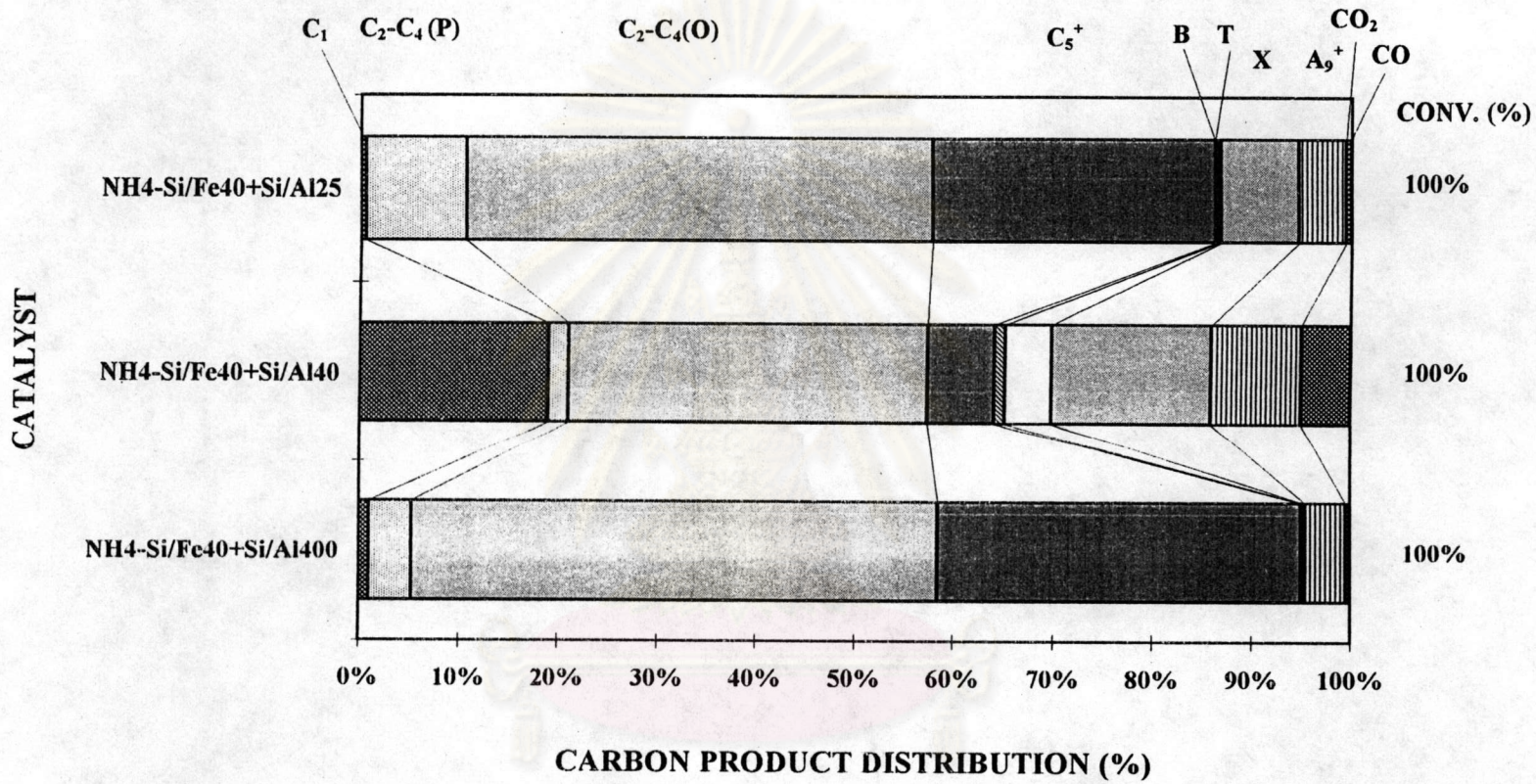

Figure 5.8 Methanol conversion on NH_4-Fe.Al-silicate with fix Fe and various Al loading content.

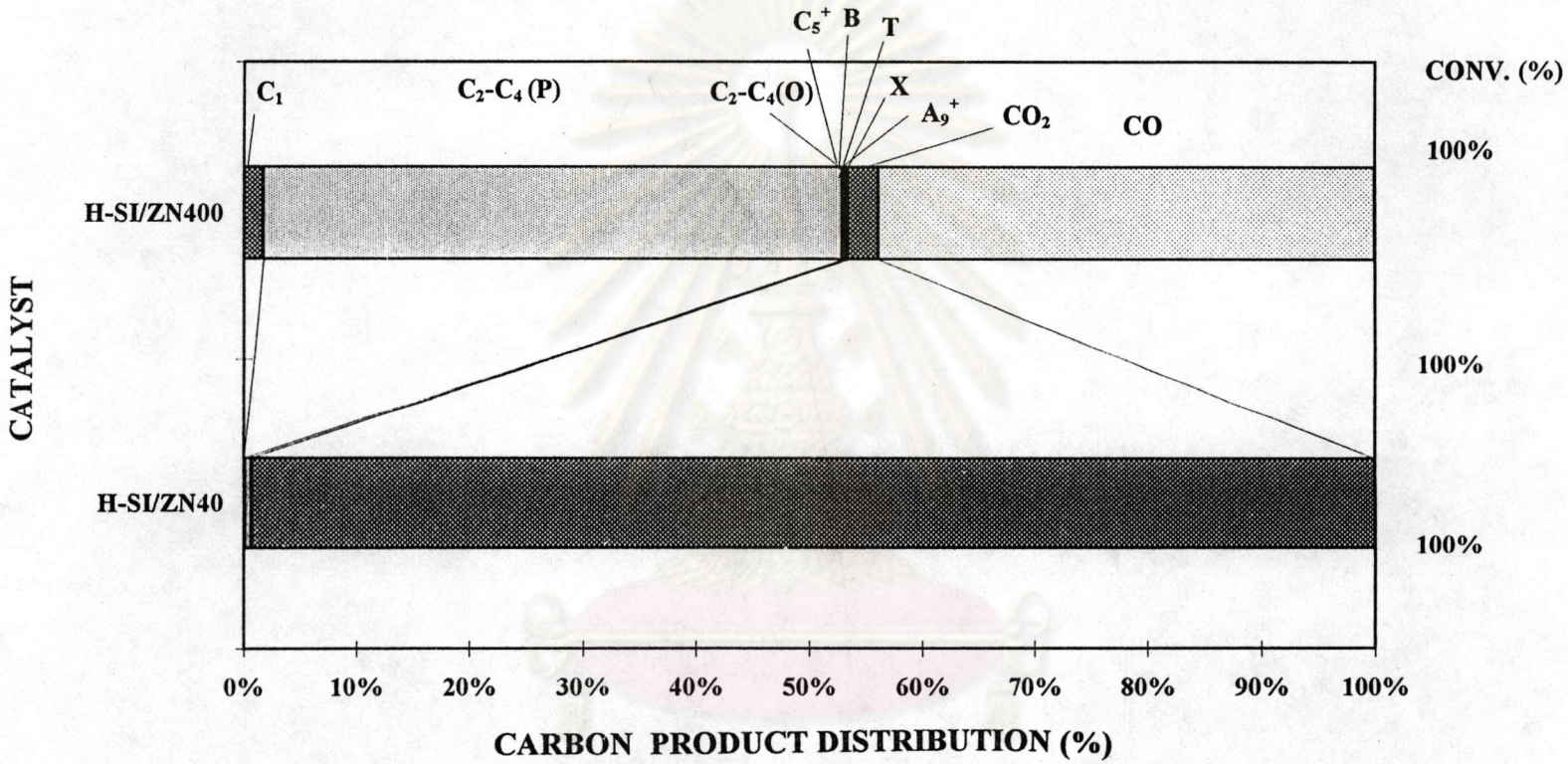

Figure 5.9 Methanol conversion on H-Zn-silicate catalysts with various Zn loading.

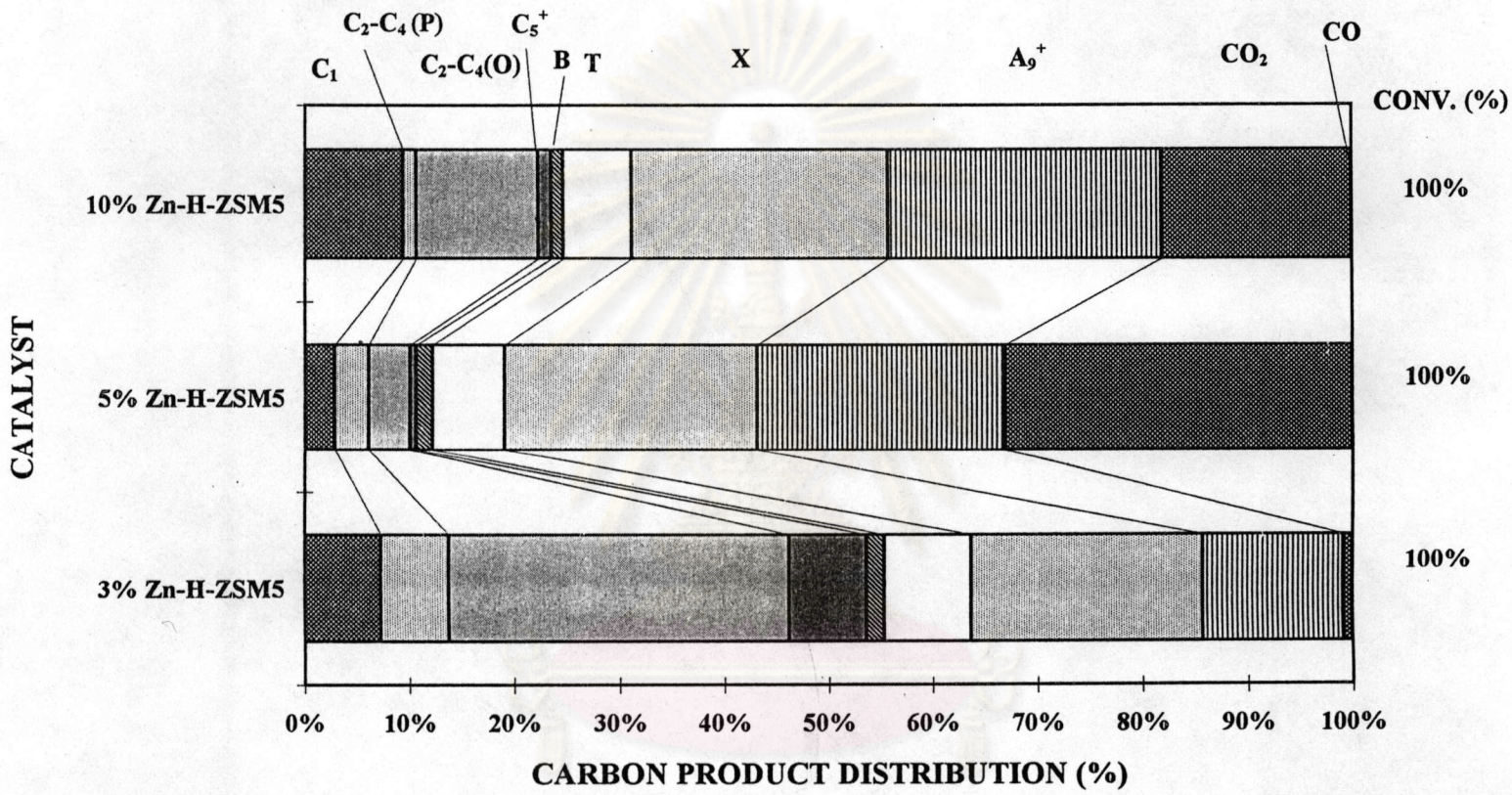

Figure 5.10 Methanol conversion on Zn/H-ZSM-5 catalysts with various Zn loading content.

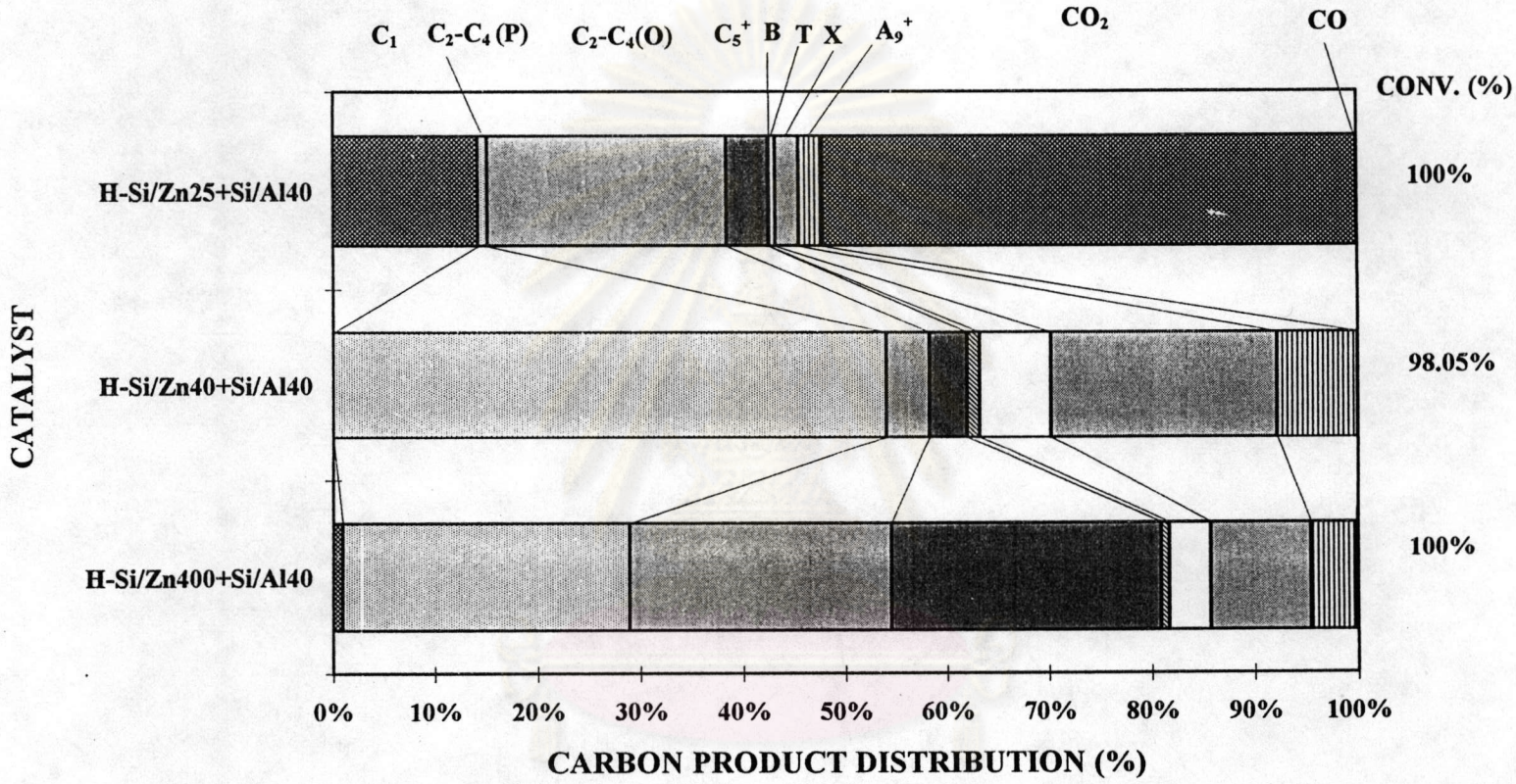

Figure 5.11 Methanol conversion on H-Zn.Al-silicate catalysts with fix Al and various Zn loading content.

silicate with Si/Zn and Si/Al ratios of 40 represents the optimum composition for the catalyst that should be used for the aromatics production from methanol.

5.1.12 Methanol Conversion on NH_4-Zn.Al-silicate

The carbon product distribution of methanol conversion on NH_4-Zn-.Al-silicate is shown in Figure 5.12. Sharply contrasted with the corresponding H-form as illustrated in Figure 5.13, NH_4-Zn.Al-silicate gave lower selectivity for BTX though the optimum formula still be the catalyst with Si/Zn and Si/Al ratio of 40.

Of all the catalysts prepared, H-Zn.Al-silicate with Si/Al and Si/Zn ratios of 40 was considered as the most proper catalyst for methanol conversion to aromatics.

5.1.13 Effect of reaction temperatures on carbon product distribution

Temperature dependence of carbon product distribution of methanol conversion on H-Zn.Al-silicate with Si/Al and Si/Zn ratios of 40 is shown in Figure 5.14. The BTX selectivity increased with the increasing temperature and as high as 37% BTX was obtained at 500° C reflecting the endothermic reaction of methanol conversion to aromatics. At temperature higher than 400° C, the considerable amount of CO_2 was formed and increased with the increasing temperature. At 600° C, the significant amounts of methane and light paraffins were formed and thus the amount of BTX decreased.

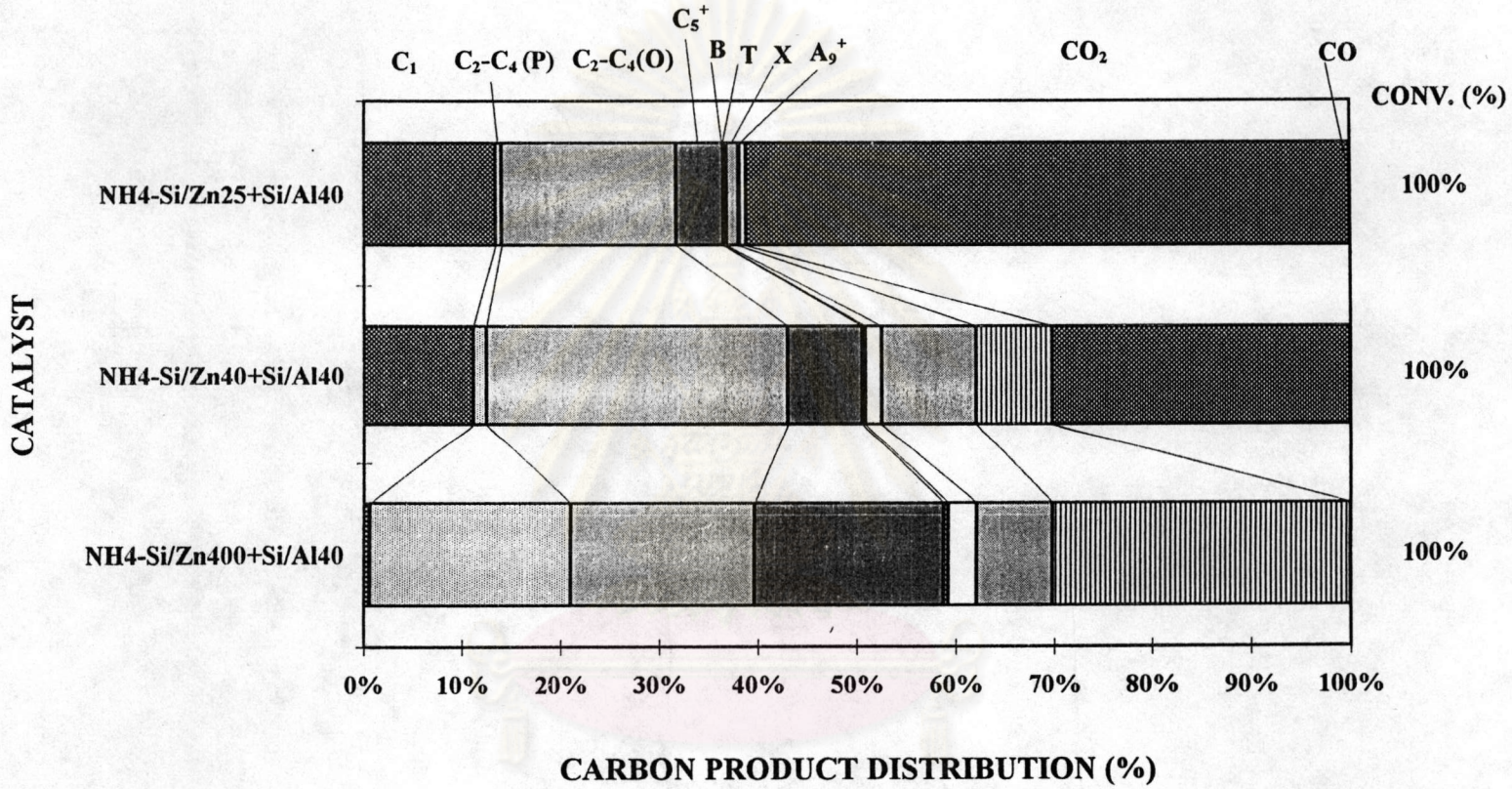

Figure 5.12 Methanol conversion on NH_4-Zn.Al-silicate catalysts with fix Al and various Zn loading content.

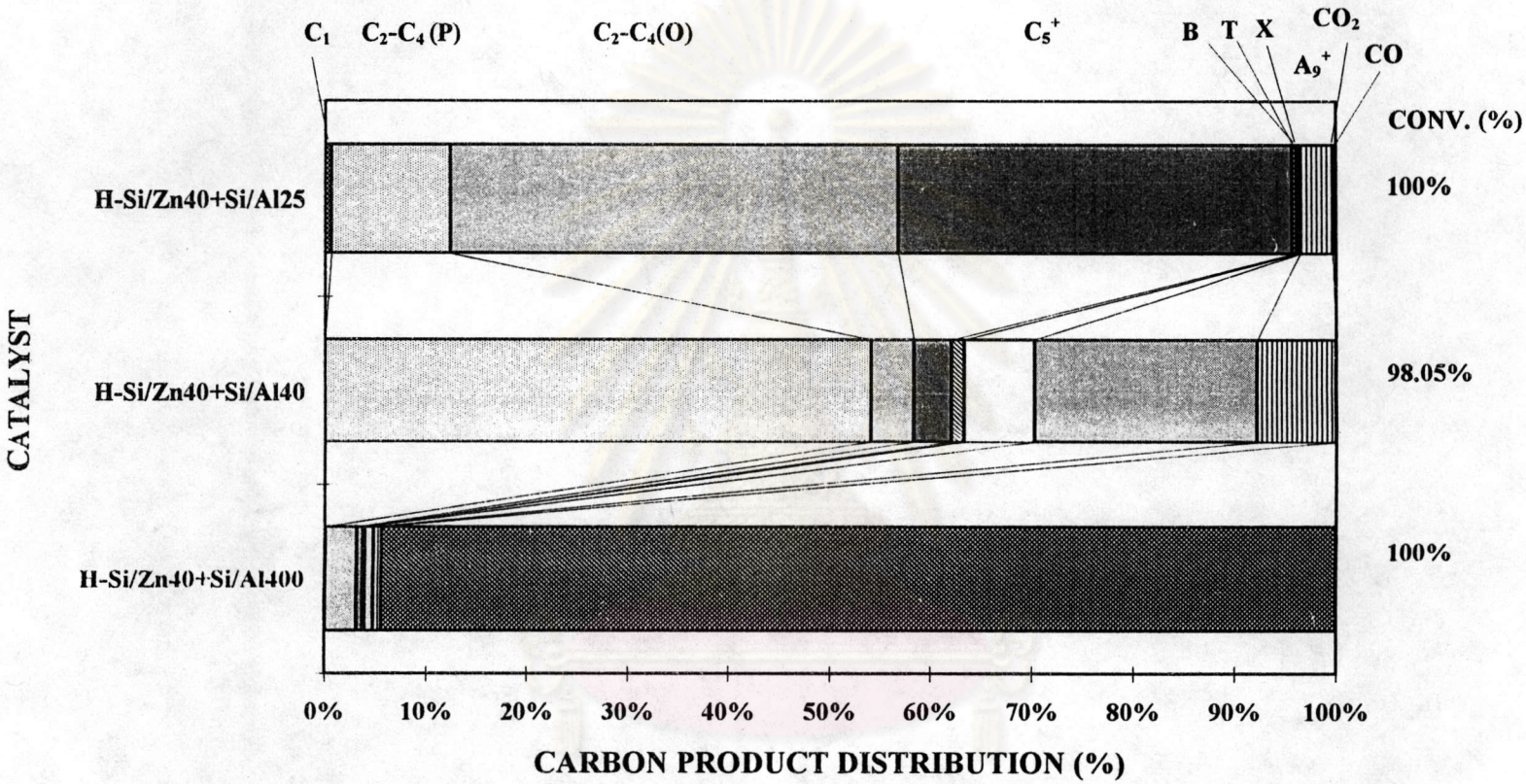

Figure 5.13 Methanol conversion on H-Zn.Al-silicate with fix Zn and various Al loading content.

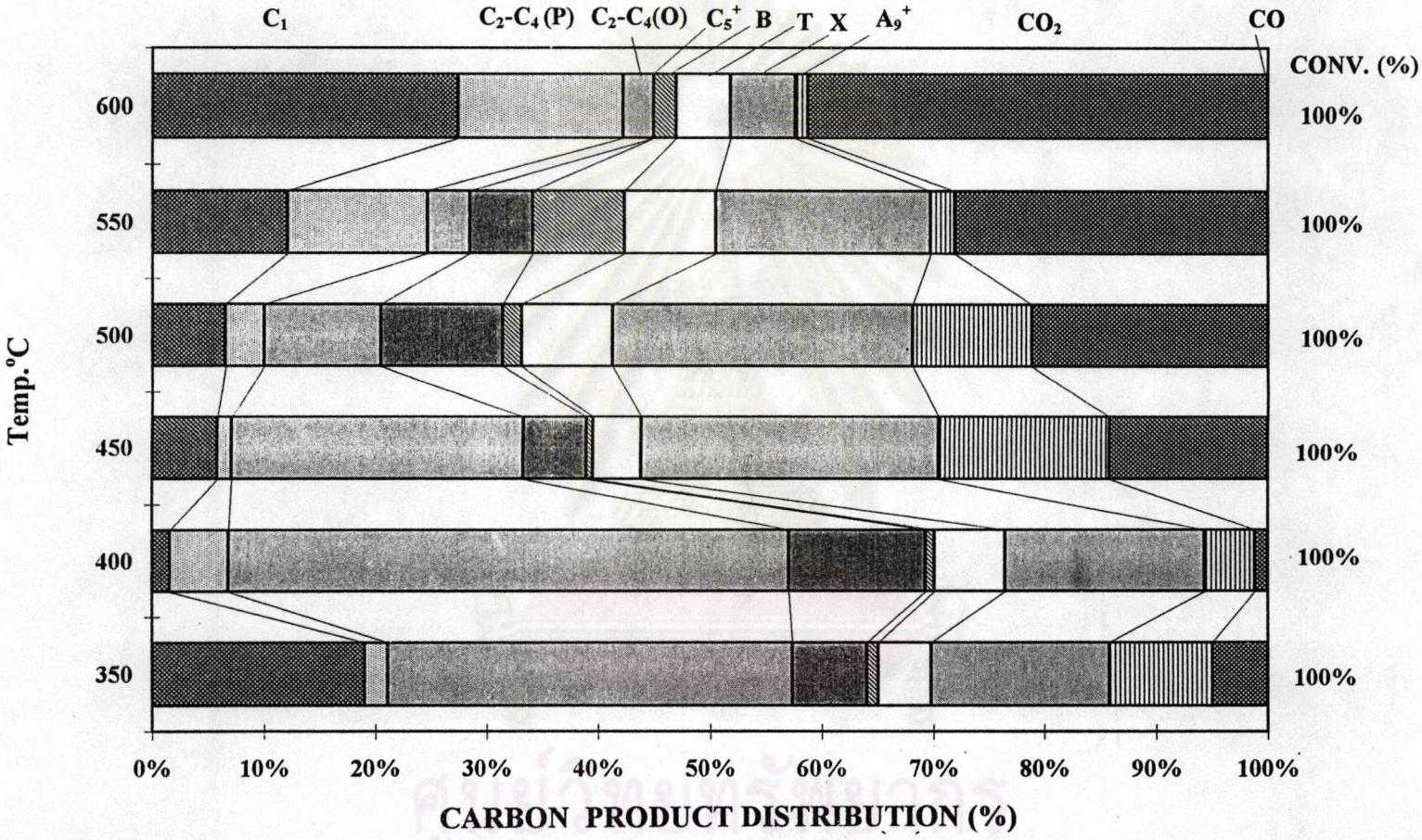

Figure 5.14 Methanol conversion on H-Zn.Al-silicate (Si/Zn40, Si/Al40) catalyst with various resetion temperature.

5.1.14 Blank test of methanol conversion

The methanol conversion reaction was conducted without catalyst to observe the thermal cracking effect at 300 and 500° C. As shown in Figure 5.15 only few amount of methanol was thermally cracked at both temperatures. It should be noted that methane was formed as the main product at 350° C and CO_2 was substantially obtained at 500° C. The result suggested that methanol may be thermally cracked to different products at relatively medium and high temperatures.

5.1.15 Effect of GHSV on carbon product distribution

The carbon product distribution at 350° C with different GHSV ranging from 2000-4000 h^{-1} is shown in Figure 5.16. It has been shown that the light olefins fraction increased with the increasing GHSV and thus the amount of BTX was less obtained at high GHSV. This should be due to the short contact time at high GHSV which caused some light olefins remain unconverted.

5.1.16 Effect of time on stream on carbon product distribution

The catalyst stability was tested by prolonged operation at 500° C and GHSV 2000 h^{-1} for 5 h according to Figure 5.17. The BTX selectivity sharply decreased after 1 h while the increasing amounts of methane and carbon dioxide were formed. However, after regenerating catalyst with air at 550° C for 1.5 h, the initial activity and selectivity were almost recovered.

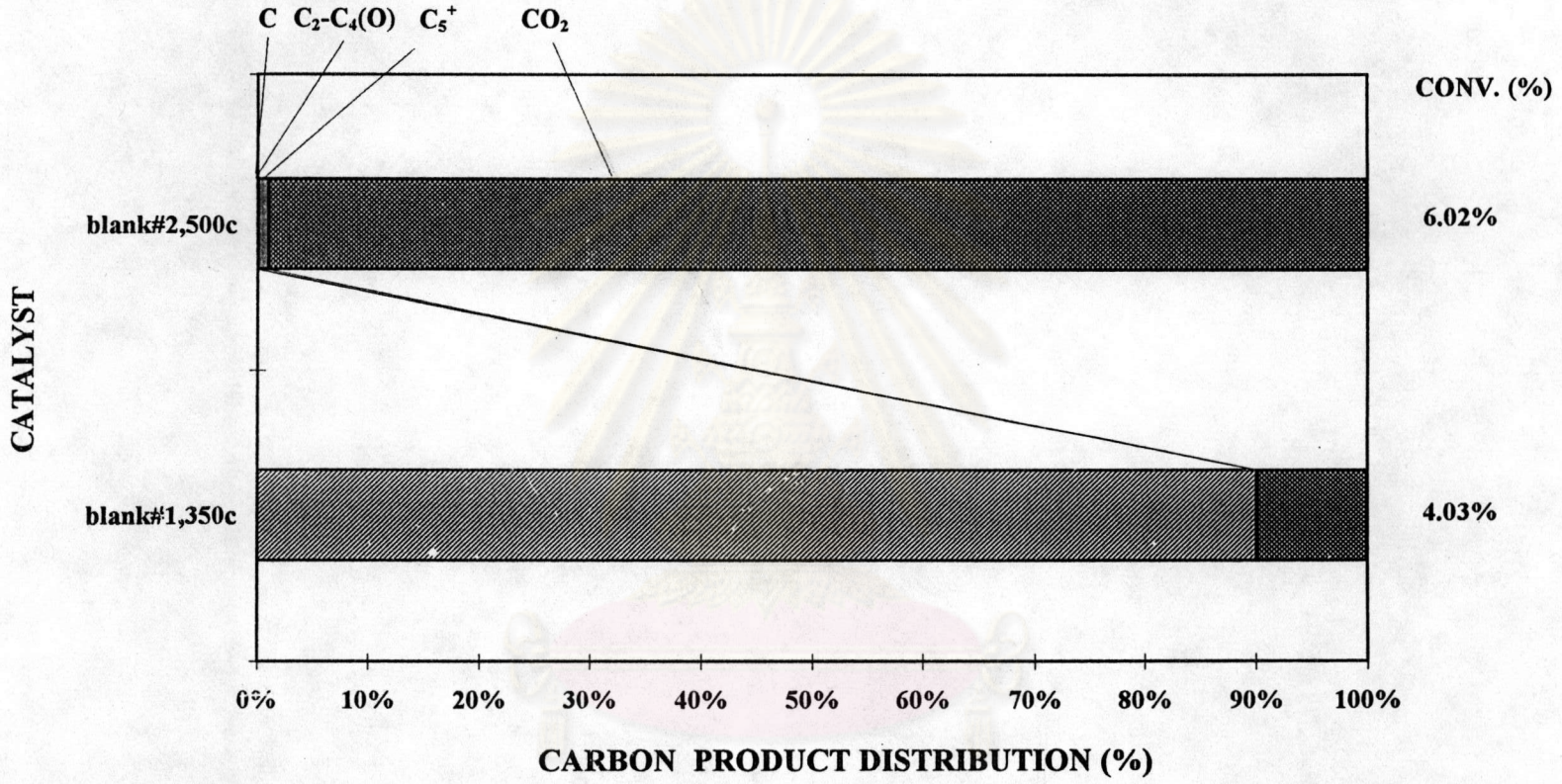

Figure 5.15 Blank test of methanol conversion without catalyst at 350 and 500° C

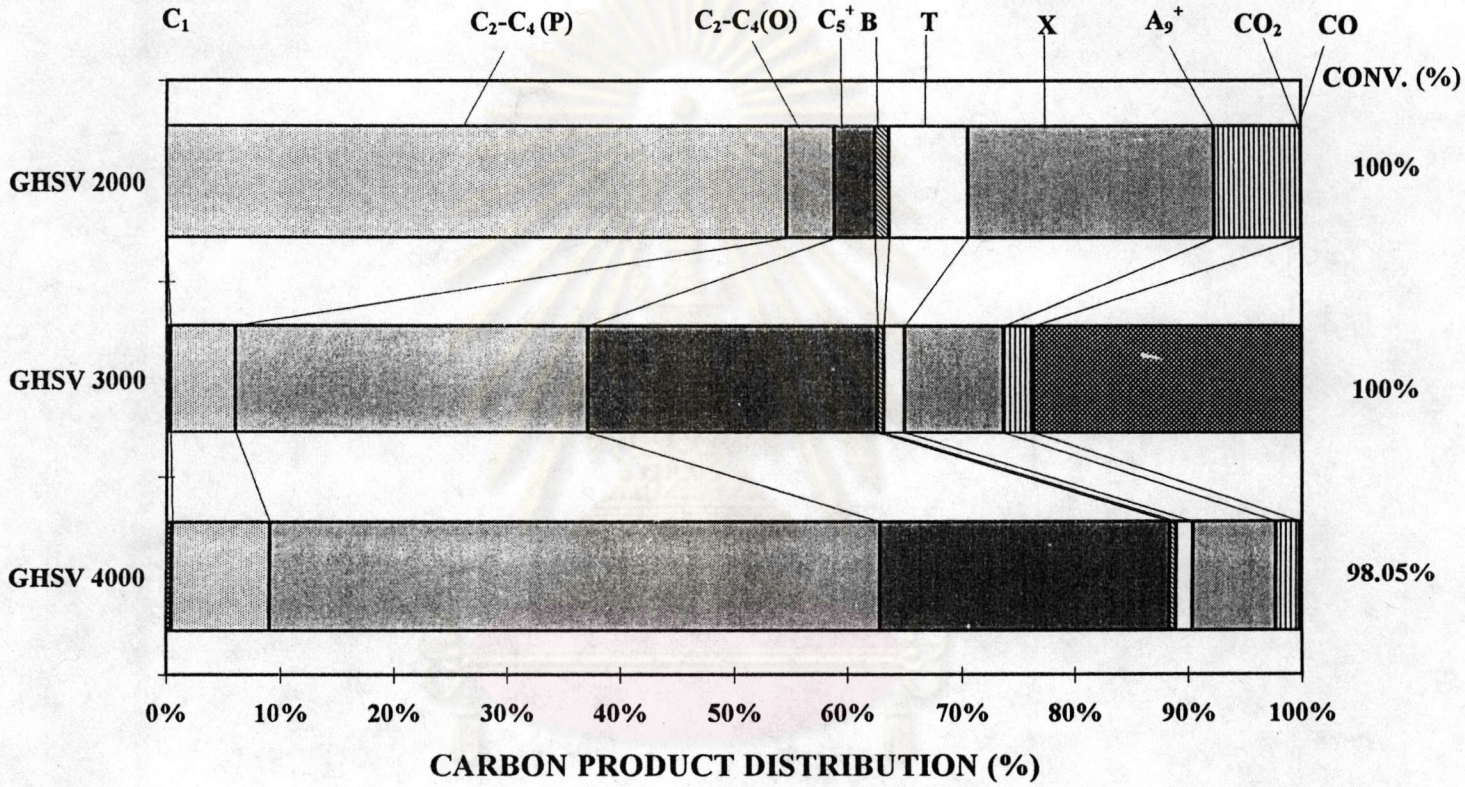

Figure 5.16 Methanol conversion on H-Zn.Al-silicate (Si/Zn40, Si/Al40) at 350° C with different space velocities

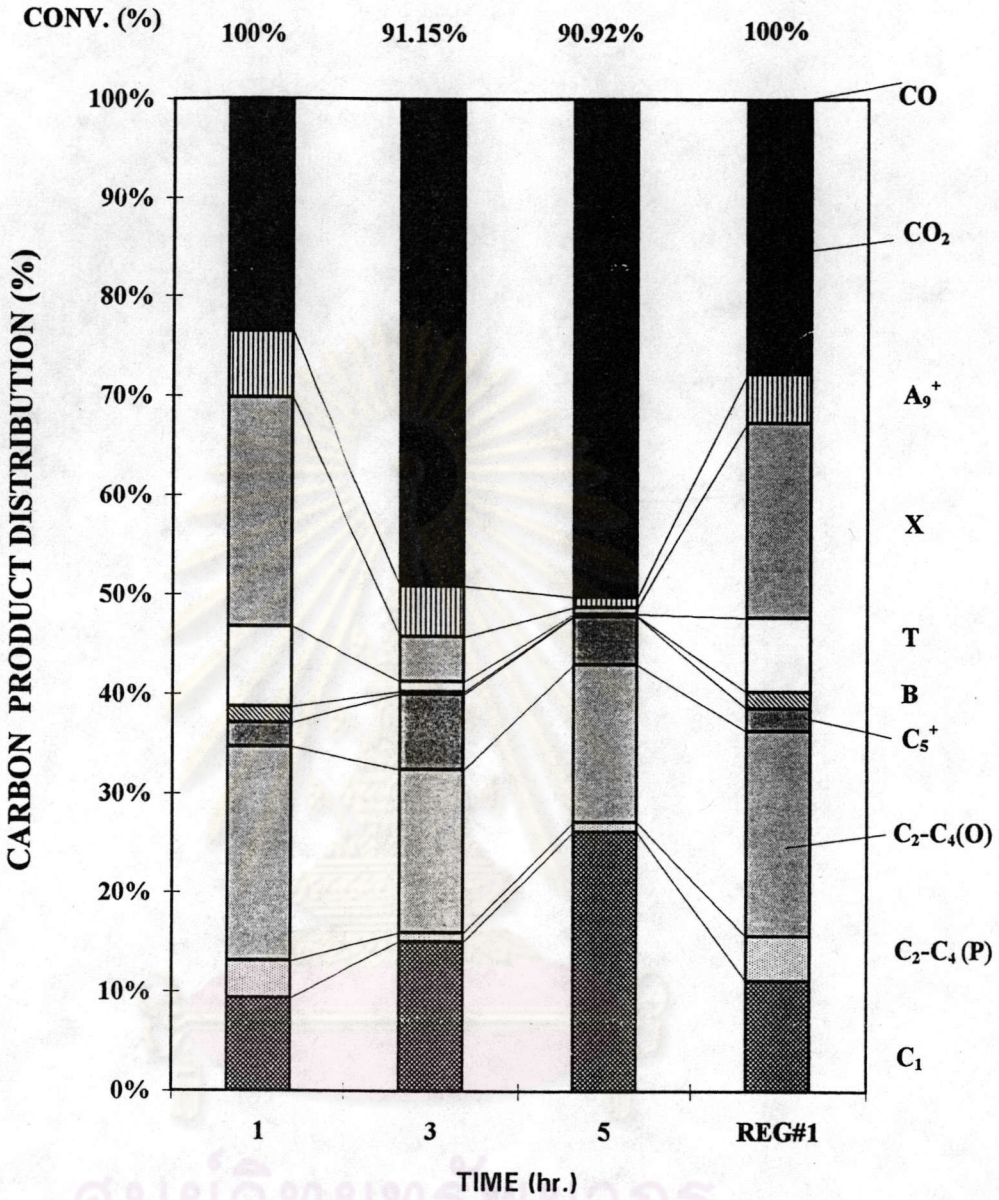

Figure 5.17 Methanol conversion on H-Zn-Al-silicate (Si/Zn40, Al/al40) catalyst at reaction temperature 500° C and GHSV 2000 h^{-1}

5.1.17 Effect of Pt on catalyst stability

The effect of Pt on catalyst stability was studied by ion-exchange H-Zn.Al-silicate with 0.5 wt % of Pt. The carbon product distribution of methanol conversion on Pt/H-Zn.Al-silicate at 500° C and GHSV 2000 h^{-1} up to 10 h is shown in Figure 5.18. Although the selectivity for BTX was not as high as that of the catalyst without Pt, the selectivity was kept almost constant at 15 % during 10 h of prolonged operation. The role of Pt as H_2 porthole, which transfer H_2 to the carbonaceous adsorbate on the catalyst surface to prevent the coke formation, as reported by Inui et al.[23] should be responsible for the catalyst stability.

From Figures 5.17 and 5.18, the significant amount of CO_2 was formed at 500° C which was also consistent with the favorable formation of CO_2 observed in the blank test. However, the increasing amount of methane was formed on H-Zn.Al-silicate without Pt after 1 h on stream while almost constant amount of methane was produced on H-Zn.Al-silicate with Pt. The author that methane might be favorably formed on the coked catalyst and further studies were required.

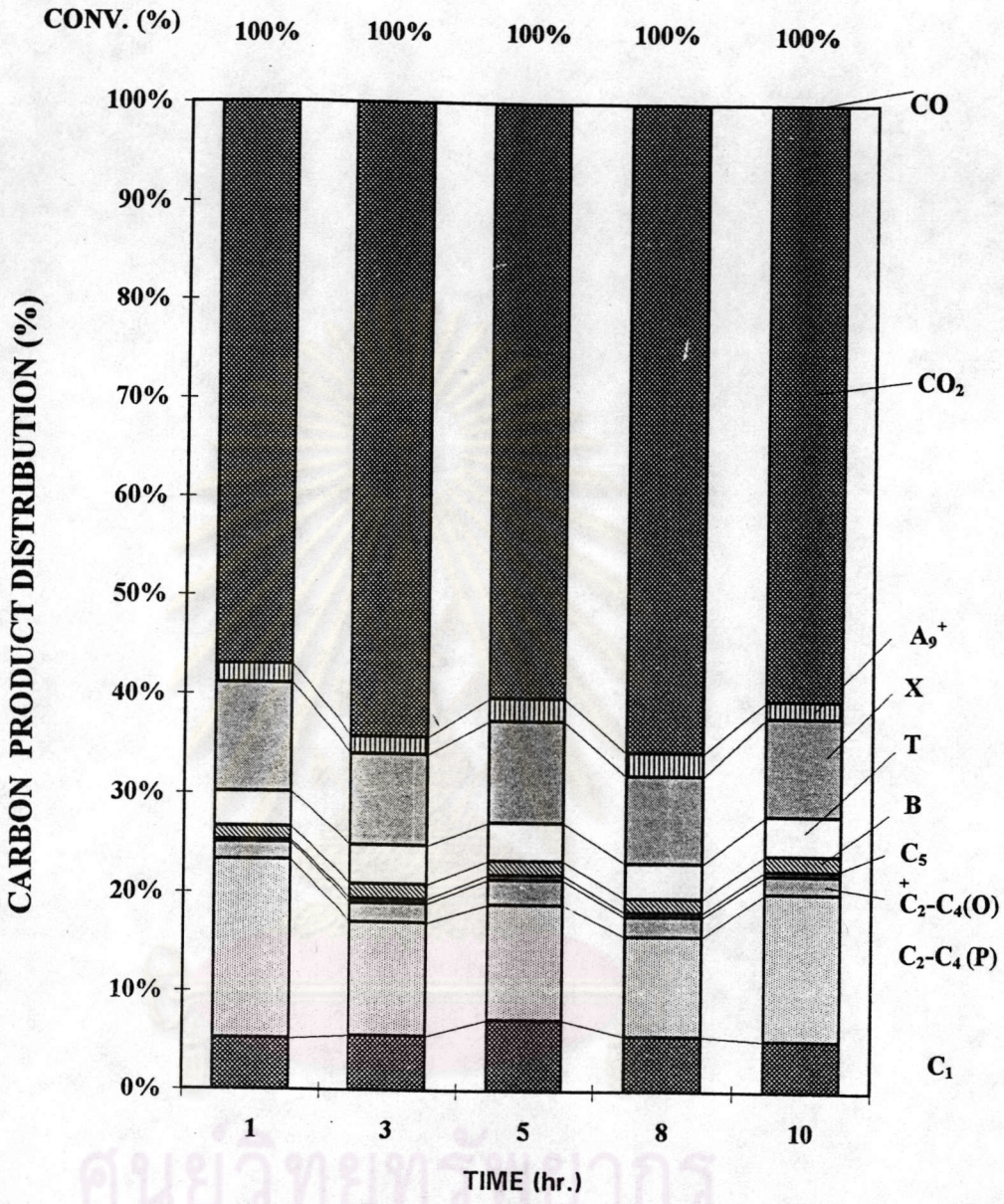

Figure 5.18 Methanol conversion on Pt(0.5 wt. %) -H-Zn.Al-silicate catalysts at reaction temperature 500°C and GHSV 2000 h^{-1}